HIGH TEMPERATURE DIGM IN AN Fe-5 at.% Al BICRYSTAL DURING Zn DIFFUSION

E.I. Rabkin, B.B. Straumal, L.S. Shvindlerman, R.A. Fournelle* and W. Gust**
    Institute for Solid State Physics, Chernogolovka, Moscow District, 142432 U.S.S.R.
 *Dept. of Mech. and Indust. Engineering, Marquette University, Milwaukee, WI 53233, U.S.A.
**MPI für Metallforschung and Institut für Metallkunde, Seestr. 75, D-7000 Stuttgart 1, Germany

Introduction

In recent studies [1,2] of the penetration of Sn and Zn along 43° <001> {001} tilt boundaries in α Fe-Si alloys and the associated premelting phase transition no migration of the boundaries was observed. Fe-Si alloys were selected for the above studies because the presence of Si guarantees the stability of the α phase over the temperature range of interest. One disadvantage of these alloys is the low solubility of Zn in them [3]. In the present study the diffusion of Zn into an Fe-5 at.% Al alloy at 850°C was examined. As for the α Fe-Si alloys, the 5 at.% Al content guarantees the stability of the α phase; however, it is not expected to result in as great a decrease in the solubility of Zn [4]. As the results below will show, however, the penetration of Zn along a 43° <001>{001} tilt boundary in the Al containing alloy, unlike the penetration of Zn in the Si containing alloys, results in the extensive (~ 100 μm) migration of both the boundary and the thin liquid film of the wetted layer immediately above it by diffusion induced grain boundary migration (DIGM) [5] and liquid film migration (LFM) [6], respectively. Also a layer of recrystallized grains, presumably formed by diffusion induced recrystallization (DIR) [5], is observed to form on the surface. Because 850°C is a relatively high temperature for the alloy in this study, extensive volume diffusion is observed ahead of the migrating boundaries and liquid films. In this study the morphology of the above reactions was characterized and the diffusion profiles associated with them were analyzed to determine both the volume and grain boundary diffusivities of Zn in the alloys.

Experimental

The 43° <001>{001} tilt boundary bicrystal of Fe-5 at.% Al alloy used in the present study was grown at a rate of 1 mm/min by electron beam zone melting in a vacuum of 1.3×10^{-4} Pa from an alloy prepared from appropriate amounts of 99.99 % Armco Fe and 99.99 % Al. The approximately 12 mm dia. x 50 mm long bicrystal was then cut into 1.5 mm x 1.5 mm square specimens between 6 and 12 mm in length by spark erosion in such a way that the boundary was in the middle of the long dimension of each specimen and perpendicular to it. Also two opposite surfaces were oriented so that the [001] tilt axis was perpendicular to them. The misorientation angle of the two halves of the bicrystal about the tilt axis was determined by both laser optical and Laue back reflection X-ray techniques with an accuracy of ± 0.5°. After mechanically grinding the long surfaces of the specimens and chemically polishing them in an 80% H_2O_2, 14% H_2O and 6% HF solution, a 100 - 150 μm Zn layer was applied to the two opposite surfaces perpendicular to the tilt axis by first immersing the specimen in a melt of 99.998% Zn at about 500°C. Then the Zn layer was ground from the surfaces parallel to the tilt axis and the excess zinc on the surfaces perpendicular to the tilt axis was partially removed by grinding until a 100 - 150 μm thick layer remained. These specimens were then encapsulated in evacuated ($< 4 \times 10^{-4}$ Pa) silica tubes and annealed at 850°C for 23 h in a tube furnace maintained within ± 2°C.

The annealed specimens were mounted in Wood's metal and ground and polished through 1 μm diamond paste. For metallographic examination the specimens were etched in a 1% solution of HNO_3 in ethanol. For electron probe microanalysis (EPMA) surfaces were first etched to reveal the grain boundary location, after which the boundary location was marked with a microhardness indentation and the surface was repolished.

EPMA measurements were carried out by wave length dispersive analysis on a JEOL 6400 electron probe microanalyzer operated at 15 kV. The intensities of the AlK_α and ZnK_α peaks were

determined using TAP and LiF crystals, respectively, and from them the Al and Zn concentrations were obtained utilizing a program, which applied both ZAF and background corrections. For the determination of the concentration profiles the beam was stepped at 1 to 5 μm intervals.

Results and Discussion

As can be seen in Fig.1(a), which shows a cross section of a bicrystal perpendicular to its tilt axis, the boundary and what at the annealing temperature had been a thin liquid film, which wet the boundary up to point B, migrated about 100 μm to the right during annealing. The migration of both boundary and liquid film were greatest at a depth of about 100 μm below the Zn coated surface with little migration of the liquid film being observed near the surface and the migration of the boundary tapering off with increasing depth below the surface until essentially no migration was observed at depths greater than 200 μm. As can also be seen in Fig.1(a) a layer of recrystallized grains formed near the Zn coated surface to a depth of about 50 μm. This depth of growth corresponds to the length of the liquid film segment near the surface which essentially did not migrate. An almost identical boundary migration and recrystallization occurred on the other zinc coated surface of the specimen.

Fig.2 shows the Zn concentration profiles taken from the regions indicated in Fig.1(b). As can be seen from Fig.2(a) the profile c(x,y) (y = const.) across a segment of the migrating grain boundary along a line from Series 1 in Fig.1(b) shows that extensive diffusion occurred up to about 60 μm ahead of the migrating boundary and that extensive interdiffusion of Zn and Fe occurred across the plane corresponding to the initial position of the boundary. Within the region left behind the migrated boundary the Zn concentration remained fairly constant at about 11 at.% at this depth. This enrichment of the material left behind the migrated boundary in Zn plus the morphology of migration shown in Fig.1(a) strongly suggest that the boundary and liquid film have migrated by DIGM [5] and LFM [6], respectively.

From Fig.2(b), which shows the Zn concentration profile through the recrystallized layer along a line from Series 2 in Fig.1(b), it can be seen that the Zn concentration is fairly constant through the recrystallized grains at about 28 at.% Zn, although it exhibits some statistical scatter about this value. Beyond the boundary of the last recrystallized grain there is a gradual drop-off in the Zn concentration with increasing depth. These observations are indicative of DIR [5], however, DIR with appreciable volume diffusion ahead of the last grain in the DIR layer.

Fig.2(c) shows the Zn concentration profile along the migrating boundary segment BCD, which was obtained from the Zn profiles along the lines in Series 1 in Fig.1(b). As can be seen, the Zn content drops off almost linearly with increasing depth.

As a final note with respect to concentration measurements it should be pointed out that the Al content along the various profiles was constant, indicating that Al did not play a role in the observed DIGM, LFM and DIR.

It is not surprising that DIGM and LFM occurred in the α Fe-5 at.% Al alloy during the diffusion of Zn, in that it has been known for some time that DIGM of grain boundaries in α Fe occurs when Zn is diffused along them [7-10]. However, it is difficult to explain why DIGM and LFM were not observed in an α Fe-5 at.% Si bicrystal having the same type of grain boundary as the bicrystal of the present study [1]. The addition of Si to α Fe decreases the lattice parameter, while the addition of Zn increases it [11]. Thus, according to the coherency strain theory [12] the coherency strain developed as the result of Zn diffusion in front of a migrating boundary should be greater for the Fe-5 at.% Si alloy than for pure α Fe, and DIGM and LFM should be more likely to occur. Al, on the other hand, like Zn, increases the lattice parameter of α Fe. Thus, according to the coherency strain theory one would expect the Fe-5 at.% Al alloy to have less coherency strain and, hence, less of a tendency to exhibit DIGM and LFM than pure α Fe or the Fe-5 at.% Si alloy during Zn diffusion. Thus, the coherency strain theory does not seem to explain the fact that DIGM and LFM do not occur in the Fe-5 at.% Si alloy.

Considering the large amount of volume diffusion observed ahead of the migrating grain boundary in Fig.1(a), the boundary migration can be classified as the high temperature form of DIGM described by Tashiro and Purdy [13]. Until recently most reports of DIGM involved boundary migration at such low temperatures that little if any volume diffusion of the diffusing element occurred in advance of the migrating boundary [5]. In fact in the studies of DIGM in α Fe resulting from Zn diffusion [7-10] the highest temperature for which DIGM was reported was 650°C [8]. For these temperatures the diffusion distance of Zn into the grain ahead of the migrating grain boundary given by D/v, where D is the volume diffusion coefficient of Zn and v is the boundary migration velocity, is estimated to be less than 0.2 nm [8], thus indicating that little if any volume diffusion occurred ahead of the migrating boundaries in these studies. However, a
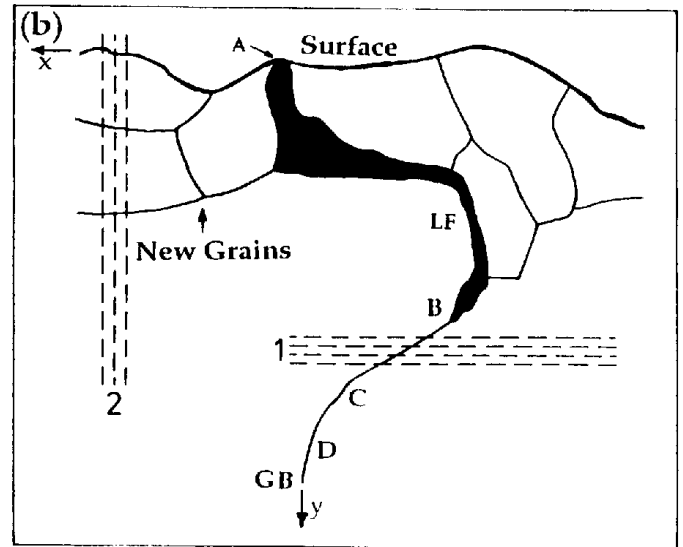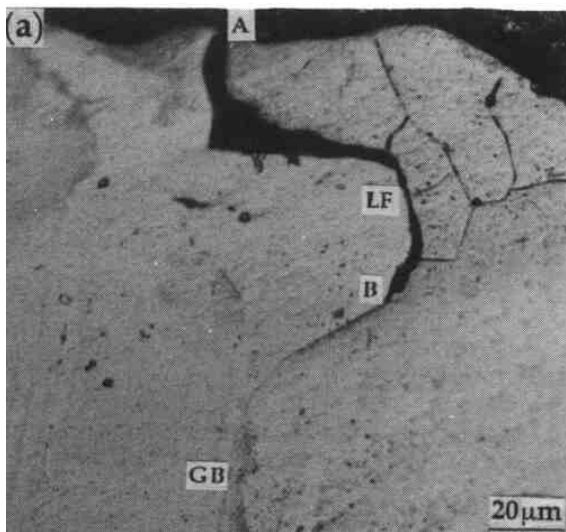
FIG.1

(a) Photomicrograph of a specimen cross section perpendicular to the tilt axis of the 43° <001>{001} tilt boundary showing wetting of the boundary from point A at the zinc coated surface to point B and migration of liquid film (LF) and the grain boundary (GB) immediately below it. A layer of new grains presumably formed by diffusion induced recrystallization (DIR) is observed near the Zn coated surface. 850°C for 23 h. (b) Schematic diagram of (a) showing the locations of concentration profile measurements.
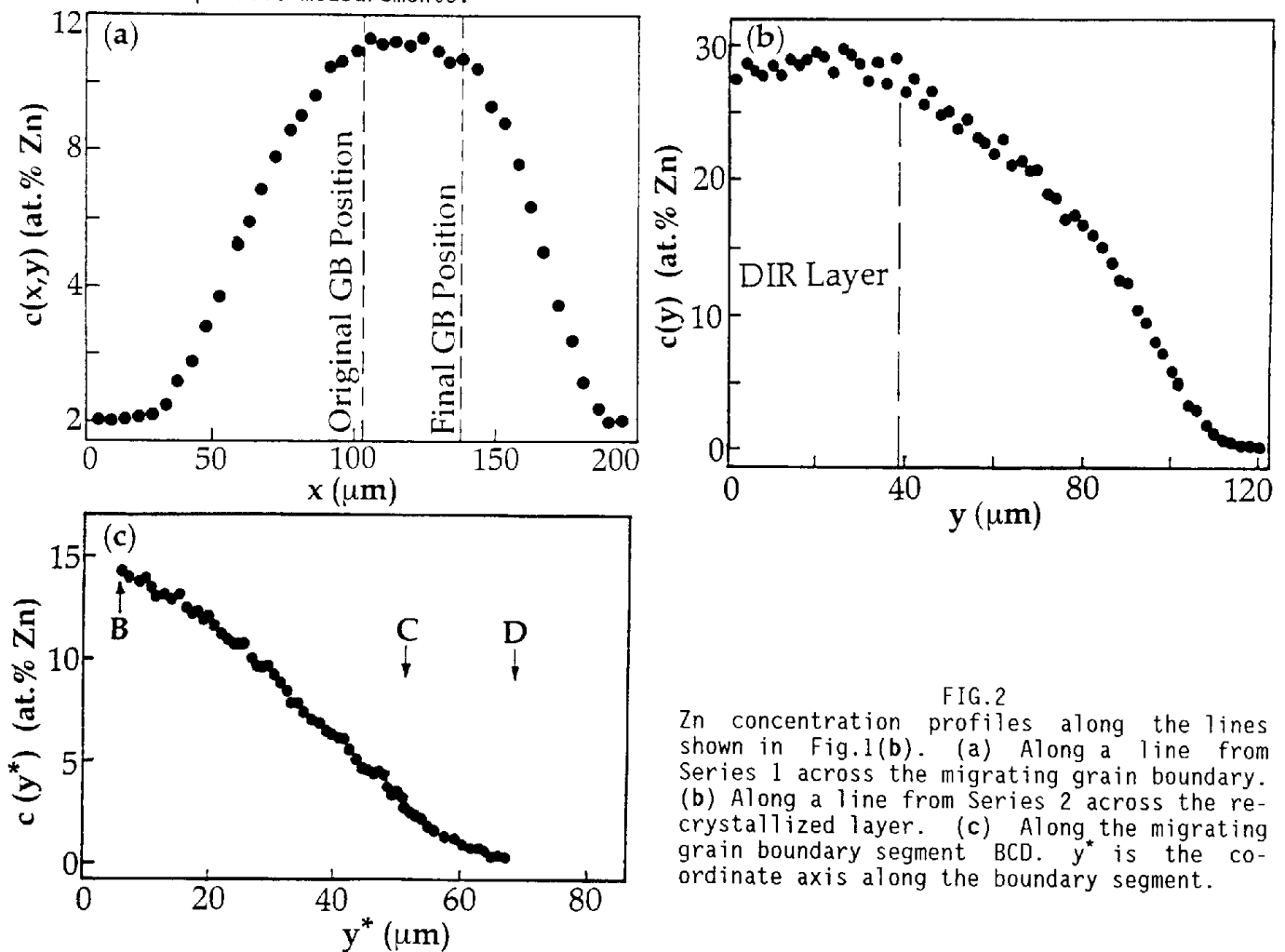
FIG.2

Zn concentration profiles along the lines shown in Fig.1(b). (a) Along a line from Series 1 across the migrating grain boundary. (b) Along a line from Series 2 across the recrystallized layer. (c) Along the migrating grain boundary segment BCD. y^* is the coordinate axis along the boundary segment.

recent analytical electron microscopy study [14] of DIGM in Ni resulting from Cu diffusion at relatively high temperatures has shown that DIGM can occur under conditions in which appreciable volume diffusion occurs ahead of the migrating boundary.

With respect to DIGM and LFM a few final comments are worth mentioning. First, the simultaneous migration of the thin liquid film and the boundary in Fig.1(a) by LFM and DIGM, respectively, is also not unexpected, as Baik and Yoon [15] have shown that the two reactions can occur simultaneously with similar morphologies. Second, the fact that the liquid film did not migrate near the surface in Fig.1(a), seems to be associated with the formation of the DIR layer, which probably resulted in the loss of driving force for LFM. Finally, it should be noted that neither the liquid film nor the boundary appeared to have undergone any oscillitary motion like that reported for DIGM in α Fe during the diffusion of Zn [8].

With respect to the DIR layer shown in Fig.1(a) it can be said that morphologically it appears quite similar to that observed during the diffusion of Zn into α Fe [8]. Also, at 50 μm the thickness of the layer is somewhat greater than most values reported for α Fe. The somewhat erratic fluctuation of zinc content in the DIR grains shown in Fig.2(b) is in agreement with the results of Guan et al. [16], which show an irregular variation of the Zn content in the DIR grains formed during the diffusion of Zn into Cu. Contrary to the observations of Chongmo and Hillert [8], however, no tendency toward oscillatory motion of the leading grain boundaries of the DIR layer were observed.

In order to determine the volume interdiffusion coefficient D ahead of the migrating boundary, Mishin and Razumovski's [17] steady state solution for the problem of diffusion along and out of a boundary migrating with a constant velocity v was used to analyze the Zn concentration profile ahead of the migrating boundary (Fig.2(a)). According to the above authors a more or less steady state concentration profile of diffusant develops ahead of a migrating boundary of the type shown in Fig.1(a) whenever the boundary migrates with a constant velocity v which is at least three times greater than the effective diffusional velocity, $v_d = 2(D/t)^{1/2}$, of the diffusant atoms in the bulk. Here t is the annealing time. Under the above condition, which will later be shown to exist for the boundary in Fig.1(a) assuming that v is constant, the concentration profile ahead of the boundary is given by

$$c(x,y) = c_o \exp [- y \, (\frac{v}{s \delta D_b})^{1/2}] \, \exp \, (- \frac{xv}{D}) \, . \qquad (1)$$

In this equation c(x,y) is the Zn concentration in moles or atoms per unit volume at some distance x ahead of the migrating boundary and some depth y below the surface, c_o is the Zn concentration at the surface (y = 0), D_b is the grain boundary diffusion coefficient, s is the boundary segregation factor, and δ is the boundary width. The coordinate system is attached to and moves with the migrating boundary. From Eq.(1) it can be seen that D can be obtained from the slope of a plot of ln c(x,y) versus x by dividing the migration velocity v by the slope. Fig.3(a) shows a plot of ln c(x,y) versus x for that part of the profile in Fig.2(a)* ahead of the migrating boundary.

The segment of the boundary from which the above profile was obtained migrated 35 μm in 23 h and, as such, moved with an average velocity of v = 4 x 10^{-10} m/s. Thus, knowing the slope of the curve in Fig.3(a) to be 0.023 μm^{-1}, the volume diffusion coefficient is found to be 7.9 x 10^{-15} m^2/s. Using this value for D and 23 h for the annealing time it is found that the effective diffusion velocity v_d is 5.9 x 10^{-9} m/s, which is 14 times greater than the migration rate v. Thus, Mishin and Razumovski's condition for steady state diffusion is met.

For comparison with the above values of D, one can also determine D values from Zn concentration profiles formed at the initial position of the grain boundary along a line from Series 1 in Fig.1(b) and below the DIR grains along a line from Series 2 in Fig.1(b).

If it assumed that the grain boundary migrates rapidly away from its initial position, leaving behind a region of constant Zn composition C_o, and the atoms on both sides of the initial position of the boundary then interdiffuse, one can analyze the concentration profile in the vicinity of the former grain boundary position using the error function solution for a pair of semi-infinite solids of different compositions [18], namely,

$$c(x,t) = \frac{C_o}{2} \, [1 + erf \, (\frac{x}{2\sqrt{Dt}})] \, . \qquad (2)$$

In this equation c(x,t) represents the Zn concentration in moles or atoms per unit volume at some

---

*Note that the concentrations in Figs.2-4 are in at.% Zn and not moles or atoms per unit volume. This will not affect the analysis provided that the molar volume is constant over the concentration range studied. In the present study the molar volume varies by no more than 4%.

distance x to the left or right of the original grain boundary position after annealing for some time t. Thus, one can obtain a value for the interdiffusion coefficient D from the slope of a plot of x^2 versus $\{erf^{-1}[(2c(x,t)-c_o)/c_o]\}^2$ and a knowledge of the annealing time t. From such a plot (Fig.3(b) for the profile in Fig.2(a)) one gets a slope of 696 μm^{-2}, and from this slope and the slopes from six parallel profiles (Fig.1(b)) a value of 2.3 x 10^{-15} m^2/s was obtained for D. The success of this analysis depends on how rapidly the boundary migrates away from its initial position. The more rapid the migration, the better the results.

If it is assumed that the DIR layer forms rapidly relative to the time required for volume diffusion, then the profile formed about the final position of the DIR grain layer can also be described by the error function solution. That is, if the DIR layer forms quickly, as it does during Zn diffusion into α Fe [8], then the diffusion geometry associated with a pair of semi-infinite solids is again set up. As can be seen in Fig.3(c), relatively linear behavior results from a plot of y^2 versus $\{erf^{-1}[(2c(y,t)-c_o)/c_o]\}^2$. From the slope of this line a value of 1.4 x 10^{-14} m^2/s is obtained for D.

The values of D obtained as described above agree within an order of magnitude of the values of 3.2 x 10^{-15} m^2/s for Zn diffusion in α Fe [19] and 1.6 x 10^{-14} m^2/s for Zn diffusion in an Fe-5 at.% Si alloy [1], indicating that the assumptions used in the above analyses, while in some cases a bit crude, were realistic. The variation among the values obtained for D is, indeed, probably associated with the assumptions.

From Eq.(1) it can be seen that, if the Zn concentration profile, c(o,y), along the grain boundary is known, one can determine the grain boundary diffusivity $s\delta D_b$ from the slope of a plot
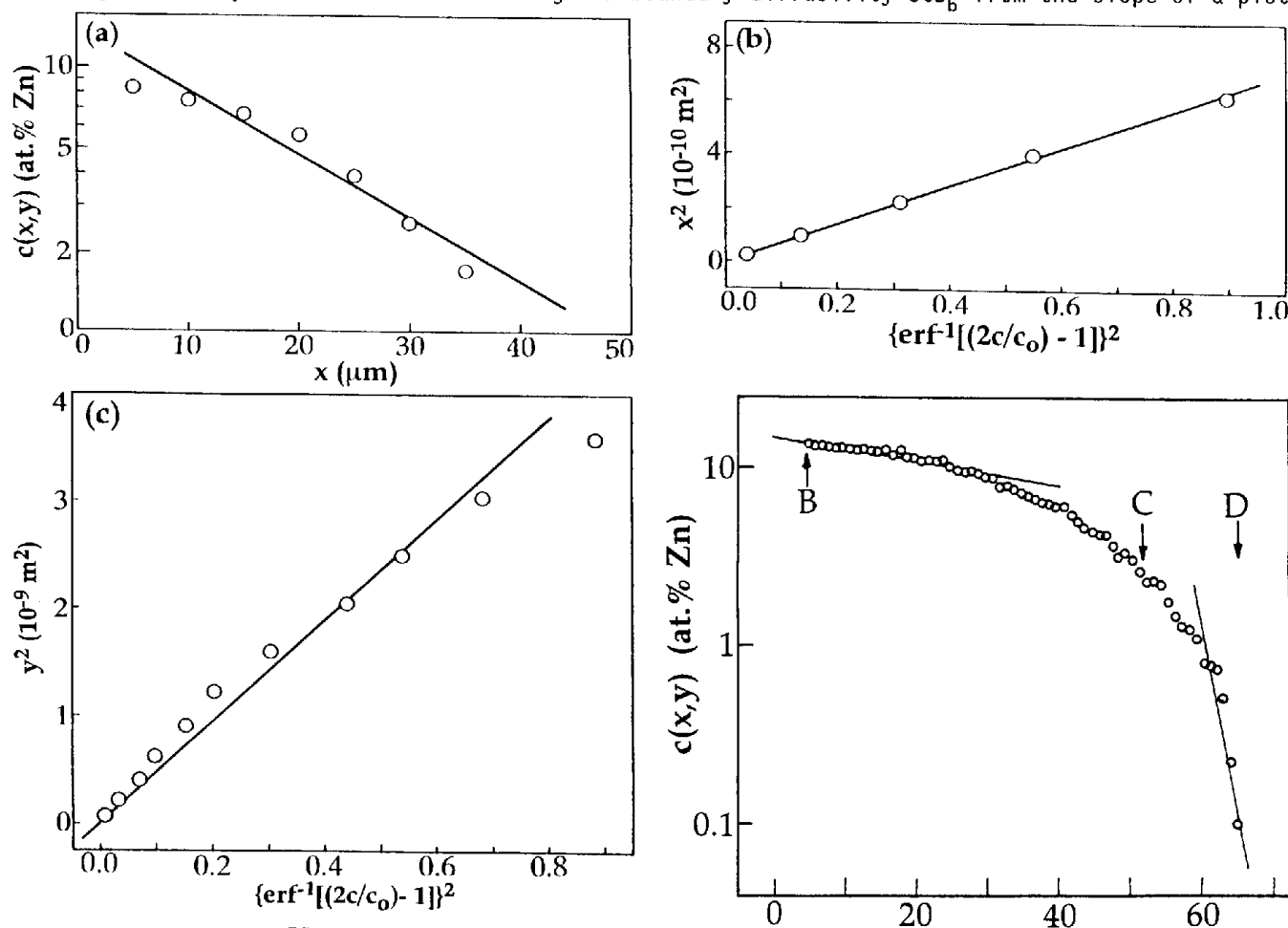

FIG.3
Analyses of the Zn concentration profiles presented in Fig.2 for D. (a) Profile developed immediately in front of the migrating boundary (Fig.2(a)). (b) Profile developed at the original position of the grain boundary (Fig.2(a)). (c) Profile below the DIR layer (Fig.2(b)).

FIG.4
Analysis of the Zn concentration profile along the migrating grain boundary segment BCD for the boundary diffusion parameter $s\delta D_b$.

of ln c(o,y) versus y and a knowledge of the boundary migration rate v. Unfortunately one does not know what the boundary Zn concentration actually is; however, one can assume that it is proportional to the Zn concentration in the material left behind the migrating boundary. With such an assumption the slope necessary for the determination of $s\delta D_b$ can be determined from a semi-logarithmic plot of the Zn concentration in the grain left behind the migrating boundary against position y along the boundary provided that the dependence is linear. Fig.4 shows such a plot for the profile shown in Fig.2(c) taken along line BCD in Fig.1(b). Here the coordinate y^* denotes position along the line BCD. As can be seen ln c(y^*) exhibits a nonlinear dependence on y similar to that observed for diffusion of Zn into α Fe-Si alloys [1,2]. As in the α Fe-Si alloys the magnitude of the slope increases with increasing distance along the boundary. This, in turn, corresponds to a large decrease in $s\delta D_b$. Unlike α Fe-Si alloys, however, no sharp transition from high diffusivity to low diffusivity is observed. As for the α Fe-Si alloys, the high and low diffusivity regions in Fig.4 were analyzed to determine values of $s\delta D_b$. In order to do this the straight lines in Fig.4 were fit to data points near the ends of the concentration profile. From the slopes of these lines and boundary migration rate values $s\delta D_b$ values were then determined. For the high diffusivity region this amounts to 1.6×10^{-18} m^3/s; for the low diffusivity region, 3.2×10^{-20} m^3/s. These values are about a factor of 10 lower than the corresponding values $(1.5 \times 10^{-17}$ and 3.0×10^{-19} m^3/s) for the grain boundary diffusion of Zn in an Fe-5 at.% Si alloy.

Conclusions

From the above results it can be concluded that high temperature forms of LFM, DIGM and DIR occur in an Fe-5 at.% Al alloy as the result of Zn diffusion at 850°C. Considerable volume diffusion of Zn ahead of the migrating liquid films and boundaries is observed, and analyses of the Zn concentration profiles associated with them delivers volume diffusion coefficients which are in reasonable agreement with published values for α iron and a ferritic Fe-5 at.% Si alloy. Analysis of the Zn concentration profiles in the material left behind the migrating boundary yielded high and low grain boundary diffusivities, which are about one order of magnitude lower than corresponding values for boundary diffusion in a ferritic Fe-5 at.% Si alloy.

Acknowledgements

References

1. E.I.Rabkin, V.N.Semenov, L.S.Shvindlerman and B.B.Straumal, Acta metall.mater. **39**, 627 (1991).
2. L.S.Shvindlerman, W.Lojkowski, E.I.Rabkin and B.B.Straumal, C.Physique, Coll.C1 **51**,629 (1990).
3. W. Köster and T. Gödecke, Z. Metallk. **59**, 605 (1968).
4. W. Köster and T. Gödecke, Z. Metallk. **61**, 649 (1970).
5. A.H. King, Int. Metall. Rev. **32**, 173 (1987).
6. D.N. Yoon and W.J. Huppmann, Acta metall. **27**, 973 (1979).
7. M. Hillert and G.R. Purdy, Acta metall. **26**, 333 (1978).
8. L. Chongmo and M. Hillert, Acta metall. **29**, 1949 (1981).
9. J.E.Blendell, C.A.Handwerker, W.A.Kaysser and G.Petzow,in Surfaces and Interfaces in Ceramics and Ceramic Metal Systems (eds. J.Pask and A.Evans), p.217, Plenum Press, New York (1981).
10. Z.-S. Yu and P.G. Shewmon, Metall. Trans. A **13A**, 1567 (1982).
11. W.B. Pearson, A Handbook of Lattice Spacings and Structures of Metals and Alloys, pp.359, 633, 634, Pergamon Press, London (1958).
12. M. Hillert, Scripta metall. **17**, 237 (1983).
13. K. Tashiro and G.R. Purdy, Scripta metall. **21**, 455 (1983).
14. D. Liu, W.A. Miller and K.T. Aust, Acta metall. **37**, 3367 (1989).
15. Y.J. Baik and D.N. Yoon, Acta metall. **33**, 1911 (1985).
16. Z.M. Guan, G.X. Liu, D.B. Williams and M.R. Notis, Acta metall. **37**, 519 (1989).
17. Yu. Mishin and I.M. Razumovski, Acta metall. mater., in press.
18. P.G. Shewmon, Diffusion in Solids, p.11, McGraw-Hill, New York (1963).
19. I. Richter and M. Feller-Kniepmeier, Phys. stat. solidi (a) **68**, 289 (1981).